Hygienic coatings with nano-functionalized diatomaceous earth by *Equisetum giganteum* – Mediated green synthesis

Leyanet Barberia-Roque [a], Marisa Viera [a,b], Natalia Bellotti [a,c,*]

[a] *Centro de Investigación y Desarrollo de Tecnología en Pinturas: CIDEPINT (FI-UNLP, CICPBA, CONICET), Argentina*
[b] *Facultad de Ciencias Exactas, Universidad Nacional de La Plata, Argentina*
[c] *Facultad de Ciencias Naturales y Museo, Universidad Nacional de La Plata, Argentina*

A B S T R A C T

Background: Microbiological growth on indoor surfaces has a negative impact on human health. Antimicrobial materials are intensely studied to prevent biodeterioration in an indoor environment. The present work seeks the green synthesis of an eco-friendly and cheap antimicrobial nano-functionalized filler from diatomaceous earth to be applied to the formulation of paints.
Methods: Adsorption of silver ions and a green synthesis with *Equisetum giganteum* L. aqueous extract of nano-functionalized diatomaceous earth was carried out. The nano-functionalized fillers were characterized by fourier transform infrared (FTIR) spectroscopy, scanning electron microscopy (SEM), transmission electron microscopy (TEM) and energy dispersive spectrometry (EDS). The antimicrobial activity was also assessed. Waterborne paints were formulated and prepared, then bioassays were performed to assess their antimicrobial efficiency.
Significant findings: For the first time *E. giganteum* aqueous extract has been employed for the nano-functionalization of diatomaceous earth (DE). Functionalized DE has the potential to prevent biodeterioration with 25 mg of silver per 100 g of paint, which has resulted in an eco-friendly alternative for hygienic coatings.

1. Introduction

Microbial growth in building surfaces is a problem that brings concern all over the world. The microbiological colonization of materials depends on different factors, such as the humidity that is concentrated in these structures, and favors the availability of water, stable temperatures, surface properties, such as roughness, and a high composition in organic compounds characteristic of each type of material [1]. Adding to this, waterborne coatings are the target for microorganism colonization due to the availability of organic components (binder, cellulosic thickener, dispersants, antifoam, etc.) and water in the composition that they can use for their metabolic processes [2,3]. Even organic biocides (antimicrobial agents) that are integrated in commercial paint formulations can be utilized as carbon sources by some microorganisms [4]. Indoor biofilm development worsens the quality of the environment due to the release of toxins, cellular fragments, allergens, volatile biogenic compounds and other chemicals. This can negatively affect people's health, especially considering that they spend approximately 85% of their time indoors [5]. Therefore, the deterioration of indoor environmental quality becomes more relevant

due to being associated with various diseases and symptoms, such as allergies, irritation of the airways, asthma, and infections [6,7]. The outbreak of the pandemic in 2020 compounded the problem even more in densely populated urban areas, considering the conditions and control of hygiene in dwellings [8]. The interest in the study of biodeterioration and its consequences on the environment, human health and structural materials has led to increased efforts in the study of alternative materials to prevent the adhesion and growth of fungi and bacteria through, for example, nanostructured surfaces and antimicrobial coatings [9,10]. These coatings have one or more antimicrobial agents in their formulation with antibacterial and antifungal activity [11,12]. Commercial biocides frequently used in coatings (carbamates and isothiazolinones) have been subject to more regulations due to their toxic and carcinogenic effect on the environment and health [13,14]. Different approaches have been followed to replace commercial biocides by other eco-friendly alternatives to obtain efficient antimicrobial paints and coatings. Some examples are hybrid materials with functional bioactive components, photoactive pigments, nanoparticles (NPs), biogenic compounds, nanostructured surfaces and encapsulation of antimicrobials in siliceous matrices [15–17]. These smart coatings react to

environmental stimuli, conferring, for example, self-cleaning, non-stick or antimicrobial properties [18]. Metallic nanoparticles have been studied due to their wide spectrum of activity and possible mechanisms, and their interaction with the microbial cells of bacteria, fungi and algae has been established [17]. AgNPs showed different cell targets due to the development their antimicrobial activity by destabilization of cell membrane, reaction with proteins and nucleic acids, alteration of electron transport, nutrient uptake, protein oxidation or membrane potential, and the generation of reactive oxygen species (ROS) [19–21]. Ag^+ ions released through the oxidative dissolution of AgNPs reinforce the biocidal activity [22].

The addition of AgNPs associated with other materials or free in coating formulations has been reported [23–26]. Most of the research reports the addition of nanoparticles associated with pigments and extenders, such as TiO_2, $CaCO_3$, ZnO, halloysites, zeolites, [23,27–31], binders [32] or sol-gel type matrices [26,33,34], with positive results for the antimicrobial activity of waterborne paints. The direct addition of AgNPs during the preparation of an acrylic paint was disadvantageous due to their reactivity [35,36]. In previous works we have studied the antimicrobial effectiveness of paints formulated with free AgNPs obtained by a green synthesis from various plant extracts and it was concluded that although they are active, strategies to enhance and maintain this activity over time must be studied [25,37,38].

The decline in the antimicrobial effectiveness of paint containing AgNPs over time has been linked to the release of the bioactive agent, caused by the oxidation of the silver ions [39]. These ions can then create soluble complexes with organic molecules. Such complexes may be leached out when the coating encounters water in settings with elevated humidity, such as bathrooms or kitchens [30]. Consequently, it is imperative to investigate methods for embedding or immobilizing the AgNPs within coatings, aiming to enhance their stability while minimizing the active silver lost and ensuring a long-term service life [40].

Due to its properties and low-cost, diatomaceous earth (DE), a natural filler, is a promising material to be associated with functional NPs. DE is a siliceous sedimentary rock and a natural geopolymer [41,42] composed of amorphous silica ($SiO_2 x nH_2O$), which has been used as a feed additive, supplementary cementing material [43,44] filler, filter material, desiccant and an insecticide to store grain [45]. It has a unique combination of physical and chemical properties, such as high porosity, high permeability, small particle size, large surface area and low thermal conductivity. These characteristics are determined by its chemical composition where aluminosilicates and iron and aluminum oxides predominate [46,47]. In 2020, the world production of DE was estimated to be 2200,000 tons, with approximately 60% being used in filtration products and the remaining 40% being used in absorbents, fillers, lightweight aggregates, among other applications [48]. In 2021, Argentina accounted for an estimated 4% of the total world production of diatomaceous hearth and it is estimated that it contains 5% of the world reserves, being among the 5 countries with the largest reserves and the biggest exporters in the world. Therefore, finding value-added uses for diatomaceous earth could be very profitable [48].

The surface, structural and chemical characteristics of DE allow a very versatile functionalization of the material [46]. The nanoporous and nanotunnelled structure of DE is a consequence of coming from fossilized cell walls (frustules) of diatoms, where the associated mineralized biomolecules determine the nanopatterned structure (nanopores and nanotunnels) [49]. In addition to this, hydroxyl groups at the surface of DE are also good reaction sites to be functionalized [50]. In this sense, the functionalization of DE has been reported with low surface energy materials employing the sol-gel method, applying fluoro- and amino-silanes as coating formulations to obtain superhydrophobic building surfaces [50,51]. Although the findings from these studies are certainly interesting, it is worth noting that the application of the sol-gel method for the functionalization of DE ultimately leads to an increase in the overall production cost. The inherent property of DE is harnessed in the current research to functionalize siliceous materials with a low-cost

and eco-friendly approach. This process begins with the alkaline activation of superficial hydroxyl groups, resulting in their deprotonation and, therefore, a negatively charged surface [52]. Subsequently, positively charged silver ions are immobilized onto these deprotonated sites through electrostatic interactions. Finally, the introduction of a vegetable extract from *E. giganteum* is employed to reduce the ions, leading to the formation of AgNPs on the material surfaces. *E. giganteum* extract has been proved in previous research to be efficient for the green synthesis of AgNPs [53]. Phytochemicals, such as equisetumpyrone, kaempferol and quercetin among other flavonoids present in the aqueous extract of *E. giganteum*, have been related to obtaining nanoparticles [25,54].

The aim of the present research was to obtain and assess a natural filler from diatomaceous earth (DE) functionalized with AgNPs synthesized by a green process to formulate antimicrobial paints. In this sense, for the first time, *E. giganteum* aqueous extract was used for the nano-functionalization of DE. This kind of product could have applications in several industries, such as pharmaceutical, food and coatings. The functionalized DE was characterized by scanning electron microscopy (SEM), fourier transform infrared spectroscopy (FTIR) transmission electron microscopy (TEM) and energy dispersive spectrometry (EDS). The assessment of the antimicrobial activity was made by the diffusion agar method with fungal (isolated from biodeteriorated coatings) and bacterial strains: *Chaetomium globosum* (KU936228), *Alternaria alternata* (KU936229), *Escherichia coli* (ATCC 11229) and *Staphylococcus aureus* (ATCC 6538).

2. Material and methods

2.1. Characterization of the diatomaceous earth

Commercial diatomaceous earth (DE) from Argentine natural deposits was used. To know the composition of the DE, X-ray diffraction (XRD) analysis was carried out. The diffractogram was obtained on a Philips 3020 diffractometer using CuKα radiation with a Ni filter (at 35 kV, 40 mA). The sweep was carried out between 3° and 70° 2θ, with a step of 0.04° and a counting time of 2 s / step. The openings of the divergence, reception and dispersion slots used were 1, 0, 2 and 1°. The diffractogram was obtained without the use of a monochromator. The identification of the mineral phases in the total rock was made with the help of the X'Pert High Score program. The identification of minerals in the total rock was carried out with the HighScore program and the quantification was carried out with the Siroquant software based on the Rietvel method of structural refinement. To verify the presence of diatom structures, a scanning electron microscope (SEM) JCM-6000 was used.

2.2. Alkaline activation

Raw DE was mixed with a 2.2 M sodium hydroxide solution in a ratio of 50 g of DE per liter of solution and heated to 100 ºC, keeping the volume constant [52]. After two hours of constant stirring, the system was left at room temperature overnight and the activated DE (DE*) was separated from the supernatant. The DE* was washed with distilled water (DW) and at the end of each wash, the solid was removed by centrifugation at 10,000 rpm (Rolco). Before discarding the water from each wash, the pH was measured. The procedure was repeated until the pH decreased to 9. Finally, the DE* was dried until constant weight.

2.3. Determination of the adsorption ratio of silver ions/DE*

Different amounts of DE* were put in contact with 70 mL of a 10^{-2} M $AgNO_3$ solution to determine the optimal ratio between the DE* and the salt solution required to adsorb as many Ag^+ ions as possible. The mixtures were kept under constant stirring in dark conditions at room temperature for 24 h. Subsequently, they were centrifuged at 10,000 rpm and the Ag^+ content in the supernatant was determined by titration
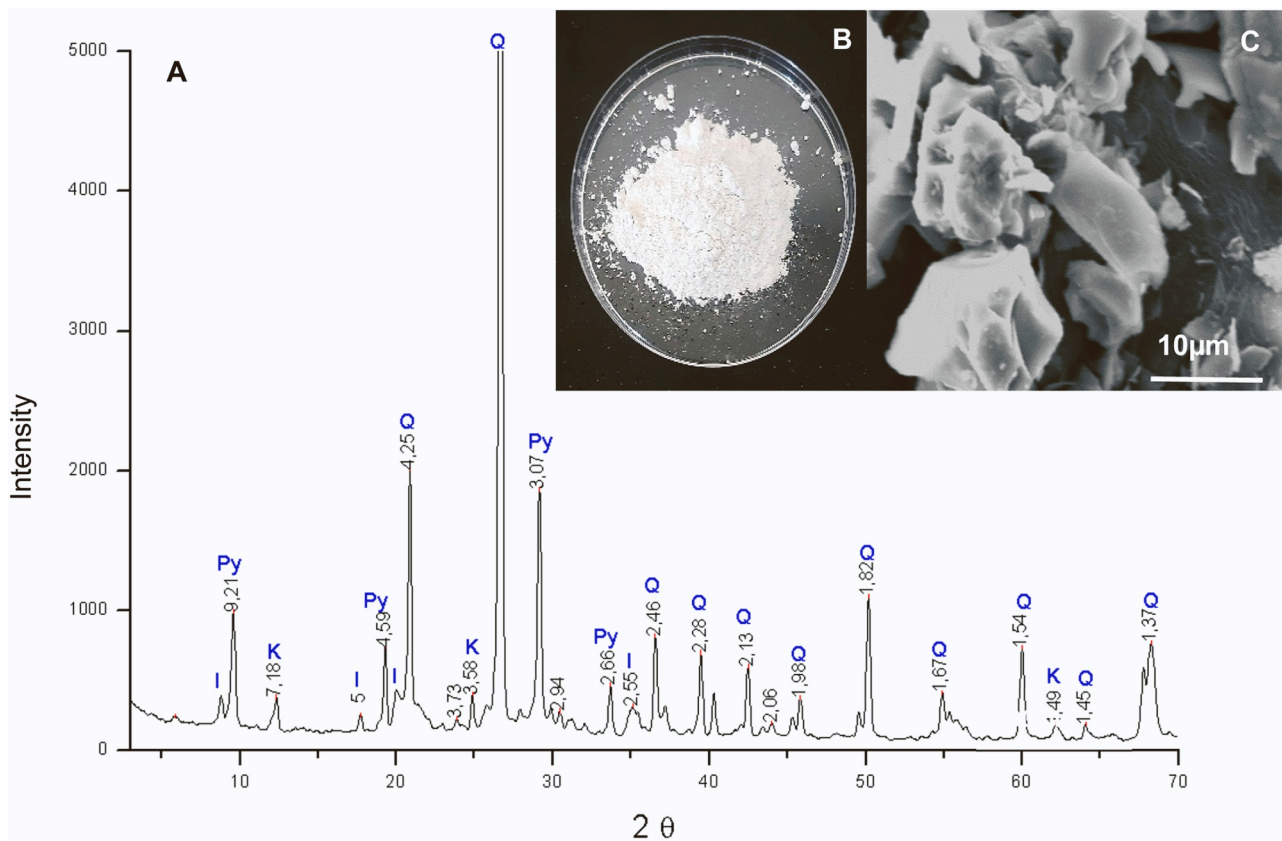
Fig. 1. (A) XRD diffractogram; (B) photographic record and (C) SEM micrograph (magnification: 3000x) of raw DE.

using the Möhr method. Adsorbed Ag^+ ions on the solids were then calculated. An optimal adsorption ratio Ag^+/DE^* was selected and it was used to continue in the next step of the functionalization. The ratio selected considered the amount of DE* necessary to adsorb the higher amount of Ag^+ in the system.

2.4. Functionalization of DE*

The solid obtained with the Ag^+ ions adsorbed was washed with DW, dried at 60 °C to a constant weight and labelled as DES. At this point, the adsorption capacity of silver no longer depends on the amount of DE in the mixture, since it has been optimized. To improve the adsorption of Ag^+ and prevent oxidation, another strategy was developed. For this, an aqueous solution (1:1) of NH_4OH was added to the silver salt solution before mixing with the DE* . This process was performed to obtain the silver diamine complex and the new functionalized DEAS. Therefore, first Ag^+ ions were adsorbed into DE* and then the vegetable extract was added to reduce the ions and obtain AgNPs on the surface. DES and DEAS were treated with aqueous plant extract from *E. giganteum*. The use of this extract was studied in previous research on the green synthesis of free nanoparticles [25]. Therefore, 10 g of each treated DE (DES and DEAS) were mixed with 5 and 45 mL of DW, following a similar methodology to that Barberia-Roque et al. for the synthesis of free Ag NPs [25]. The mixtures were kept under constant stirring in dark conditions at room temperature for 24 h and after that were washed with DW, dried at 50 °C to a constant weight and labelled as DESE and DEASE.

2.5. Characterization

DE and the functionalized DE were characterized. X-ray mapping was acquired by using a Talos F200X HR transmission electron microscope (TEM) - a dark field microscope operating at 200 kV equipped with a SuperX EDS spectrometer (composed of 4 EDS SDD detectors).

Fourier transform infrared spectra (FTIR) were obtained using the potassium bromide disk technique and a Perkin-Elmer Spectrum One spectrometer. Scanning electron microscopy (SEM) was carried out with a Philips FEI Quanta 200 coupled to an EDS detector to analyze the elemental composition and the microstructure of the solids studied. The working conditions were 6 Torr, 5 °C, 15 KV. A TEM JEOL model100 CX II was employed to analyze the size and morphology of the particles and their distribution on the surface of the material.

2.6. Antimicrobial assays

The antimicrobial activity of the functionalized DE was assessed by the agar diffusion method [55]. The culture media used for the assays were LB agar and Malt Extract (ME) agar for bacterial and fungal strains, respectively. In the case of bacterial strains, overnight cultures of *E. coli* (ATCC 11229) and *S. aureus* (ATCC 6538) in LB broth were adjusted using phosphate buffer saline (PBS) to an OD value of 0.1 at 600 nm, corresponding to 10^7 CFU/mL. The plates were subsequently seeded with the test organisms, 7 mm diameter holes were made in the culture media and they were filled with the samples and incubated at 30 °C for 24 h (RH > 90%). The fungal strains used were *Alternaria alternata* (KU936229) and *Chaetomium globosum* (KU936228), which were isolated from biodeteriorated paint films from previous research [56]. *A. alternata* grows on a wide variety of substrates and *C. globosum* is a saprophytic filamentous fungus that mainly colonizes structural materials with cellulose content [1]. After 48 h of incubation, fungal growth was observed, and the zone of inhibition was measured in the corresponding cases.

For both bacterial and fungal strains, diameters > 7 mm were considered with positive activity. Diameters = 7 were considered with antifungal activity, but without antibacterial activity. This is due to the characteristic invasive fungal growth. The statistical analysis of the results was performed by means of ANOVA with the Infostat software.
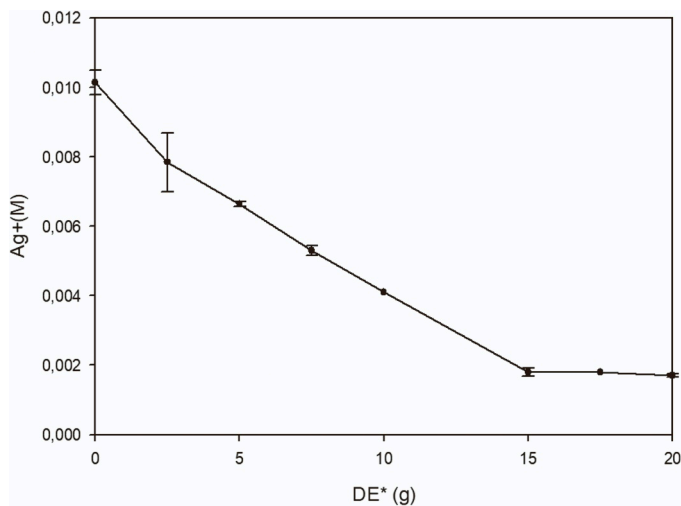
Fig. 2. Concentration of silver ions in the supernatant for different amounts of DE* .

2.7. Formulation and preparation of the paints

Waterborne paints were prepared following a conventional acrylic indoor formulation. The composition (in wt%) of the formulation paint was: 48.9% DW, 26.7% $CaCO_3$(natural), 6.0% acrylic resin, 13.0%TiO_2, 1.9% $CaCO_3$ (precipitated) and 3.5% additives (antifoaming, cellulosic thickener, dispersants and surfactants). Paints with the functionalized DE resulted from the replacement of part (6.2%) of the calcium carbonate. The control paints were labelled as: CP (basic formulation without DE) and PDE (paint with DE*). The paints with the functionalized DE (DES, DEAS, DESE and DEASE) were labelled as: PDES, PDEAS, PDESE and PDEASE. The DE concentration was adjusted considering the viscosity modification of the original paint (high viscosity makes difficult paint application) and ensuring a minimum

amount of silver, enough to be efficient against mold considering previous research [25,57].

The addition of DE in the paint was evaluated and compared with the control paint (CP) according to standards. The paints were characterized by specific weight (IRAM 1109 A2), Stormer viscosity (ASTM D562) and water absorption (ASTM D570) standard. The water absorption (in wt%) methodology relies on the determination of the difference in weight between dry samples and those exposed to a humidity chamber with an NH_4Cl saturated solution to achieve a relative constant humidity (RH) of 79.5% at 20 °C for 7 days. For the assay, sandblasted acrylic panels were painted (two layers) and allowed to dry for 24 h between each application.

Water permeability was determined by the funnel method. The paints were applied on a porous unglazed tile, after the drying and curing time, two glass funnels per sample were glued with inert sealant. Distilled water was introduced into the funnels to fill the available capacity (flush) under laboratory conditions. Then, they were weighed after different times: 24, 48 and 72 h, and by weight difference, the permeability of the film to the water was determined [58]. The hiding power was also determined according to the IRAM 1109 Standard. Color and gloss were determined on coatings employing a ByK Gardner gloss-meter. Considering CIElab parameters, L* varies from 0 to 100 (white), magenta-bluegreen (a*) and yellow-blue (b*), the change of color (ΔE) due to the incorporation of the DE was calculated [59].

2.8. Resistance of paint films to microbial growth

The antifungal efficiency of the prepared paints was evaluated by an in vitro procedure following the ASTM D5590 specification. The painted glasses, after two weeks, were cut in 2.5 × 2.5 cm squares pieces and placed in minimum mineral media. The samples were inoculated with 50 µL of a spore suspension (10^5 spores/mL) of *A. alternata* (KU936229) and *C. globosum* (KU 936228). The suspension was distributed homogeneously all over the painted surface. After four weeks of incubation at 28 °C (RH > 90%), the fungal growth was evaluated according to the ASTM D5590 standard. In this sense, the fungal growth on coatings is
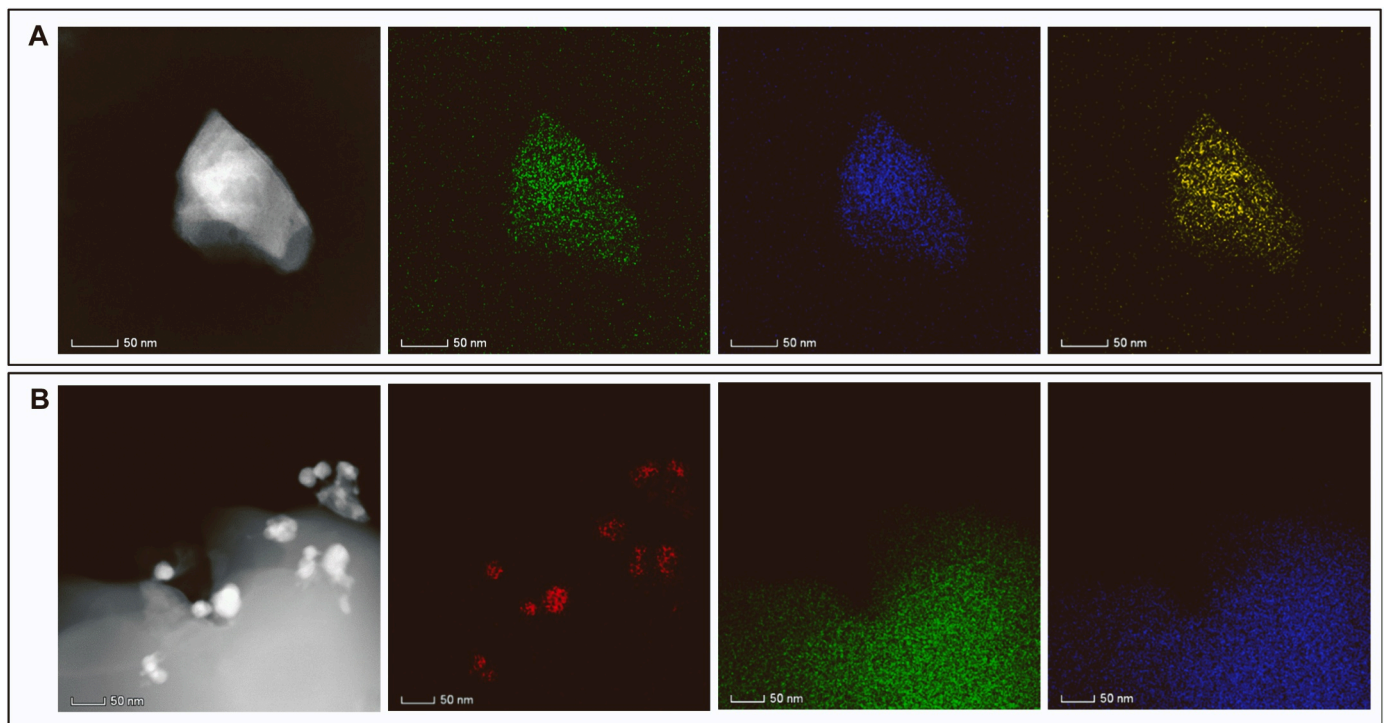

Fig. 3. TEM micrographs and EDS mapping: (A) DE and (B) DEAS. Green color is silicon, blue color is oxygen, yellow is aluminum and red is silver recount. The mapping displays the corresponding signal with the presence of silver in the sample treated with silver salt and ammonia solution (DEAS).
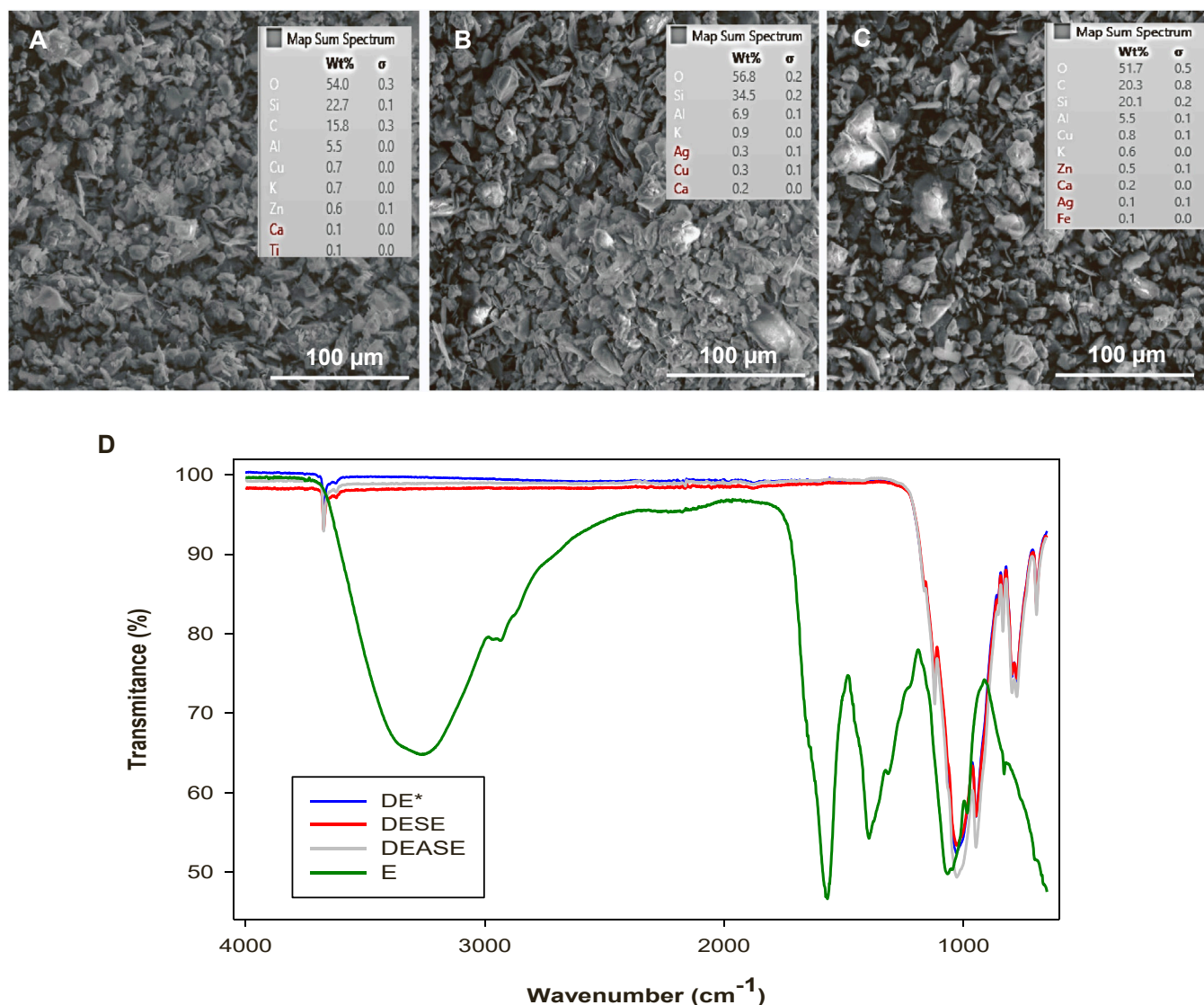
Fig. 4. SEM micrographs (magnification 1000x) and EDS elemental surface analysis: (A) DE* ; (B) DESE and (C) DEASE; (D) FTIR spectra of activated diatomaceus earth (DE*), functionalized DE (DESE and DEASE) and the aqueous extract of *Equisetum giganteum*.

referred to as the percentage (%) of area covered and rated as: 0 (none, 0%), 1 (trace of growth, <10%), 2 (light growth, 10–30%), 3 (moderate growth, 30–60%) and 4 (heavy growth, 60–100%).

3. Results and discussion

3.1. Diatomaceous earth characterization

XRD analysis of the raw DE showed that the majority component was quartz (SiO_2) at 55% and the rest of the components were pyrophyllite ($Al_2Si_4O_{10}(OH)_2$) 36%, kaolinite ($KAlSi_3O_8$) 5% and illite ($(K)(Al, Mg, Fe)_2(Si, Al)_4O_{10}[(OH)_2,(H_2O)]$) 4%. The corresponding diffractogram can be seen in Fig. 1 A. The DE studied is a white color powder and the photographic record is presented in Fig. 1B. From observations carried out by SEM, the DE microstructure presented mostly parts of the diatoms and therefore complete preserved structures were difficult to identify. In the SEM micrograph of Fig. 1 C, broken parts can be seen with the characteristic frustules pores of the DE. In this case, micron-sized pores of approximately 1.5 μm can be observed.

3.2. Functionalized DE characterization

Fig. 2 shows the concentration of Ag^+ ions in the supernatant, obtained by titration, in relation to the amount of activated DE (DE*). As can be seen in the graph, the maximum amount of Ag^+ ions adsorbed was reached at 15 g of DE* . Considering this, the amount of silver adsorbed in the DE* was calculated: as 4.04 mg Ag/g of DE. Therefore, this was the ratio that was used to obtain DES (DE*/Ag^+) and DEAS (DE*/Ag^+/NH_4OH). Observations by HR-TEM were obtained and the micrographs are presented in Fig. 3 A and B. Added to these, EDS mapping can be seen for some of the major elements (silicon, oxygen and aluminum); in the case of DEAS the signal from silver could be detected in the superficial analysis and it is highlighted in red in Fig. 3B. In the sample without treatment with ammonia solution (DES), the surface analysis did not detect a signal corresponding to silver, therefore, it was below the detection level of the equipment (0.1 wt%). Finally, with the addition of the extract from *E. giganteum* (E), DESE (DES/E) and DEASE (DEAS/E) were obtained. The SEM and EDS analysis of DE* , DESE and DEASE can be seen in Fig. 4 (A-C). No changes in the morphology of DE were observed after functionalization. The signal of silver could be detected in both functionalized samples, although in concentrations close to the detection limit of the equipment, 0.3% and 0.1%,
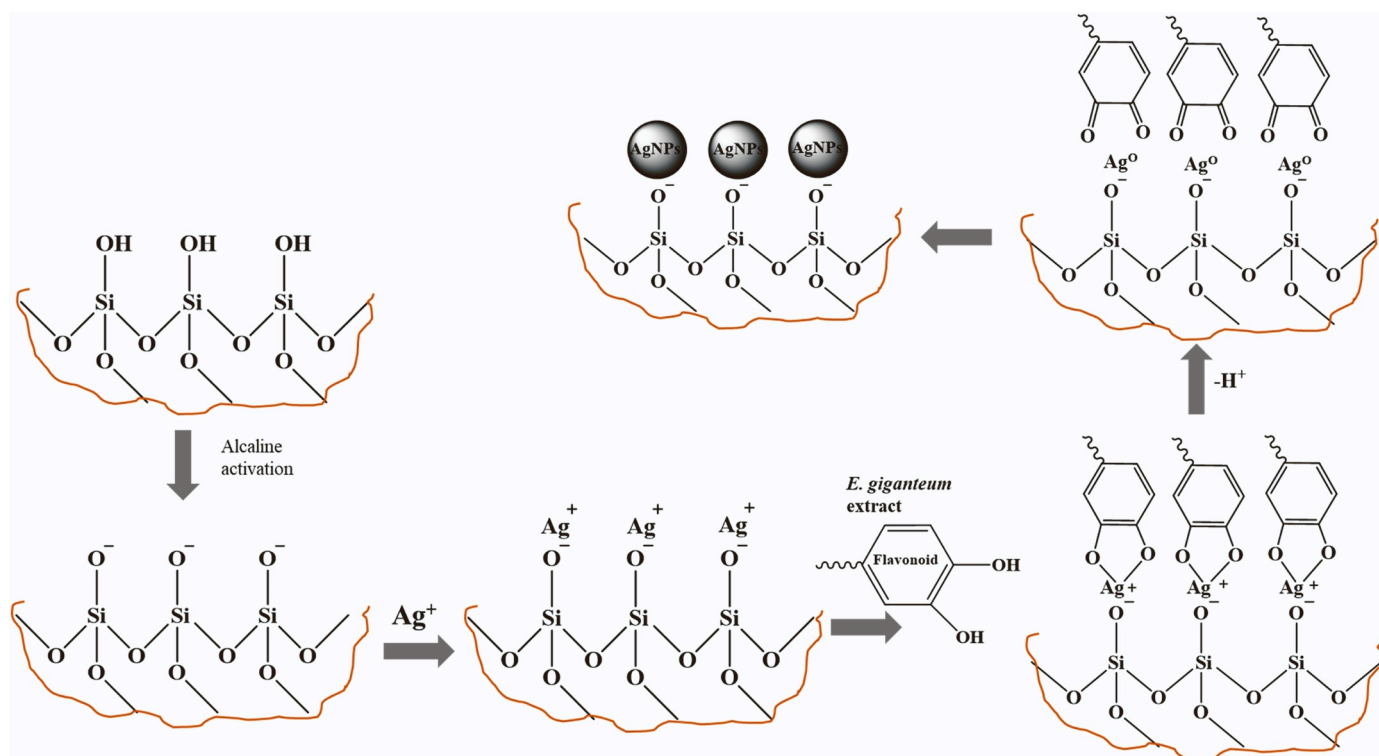
Fig. 5. Possible mechanism involved in the formation of AgNPs from *E. giganteum* extract onto diatomaceous earth.

respectively. In all the samples, the major elements were silicon, oxygen and aluminum. The presence of the phytochemicals in the process of functionalization favors the increase of the Ag element at the surface level due to the formation of nanoparticles.

The FTIR spectra obtained from DE* , DESE, DEASE and the *E. giganteum* extract are showed in Fig. 4D. The functionalized DE and DE* present similar spectra, with a characteristic peak at 1000 cm^{-1} attributed to silica (Si-O) [42]. On the other hand, the plant extract (E) show peaks at 1100, 1390, 1635 and 3300 cm^{-1} corresponding to -CH$_3$, C=O and -OH groups present in esters, alcohols, flavonoids, amides and acids [60]. The peaks are not observed in the spectra of DESE and DEASE, which could be due to the strong association established between the NPs and the siliceous support, and the elimination of the phytochemicals from the plant extract after washing process. Considering bibliographic data, flavonoids and polyphenols are strongly associated with the AgNPs' synthesis [38,61]. *E. giganteum* aqueous extract contain flavonoids, such as equisetumpyrone, kaempferol and quercetin, which have been related to NP synthesis (Francescato et al., 2013; IBB). In this sense, a possible mechanism for the functionalization of Ag NPs on DE is proposed in Fig. 5. In this proposed mechanism, Ag$^+$ ions that are adsorbed onto the activated DE surface exhibit the ability to establish intermediary complexes with the phenolic hydroxyl groups (3´and 4´position) present in the flavonoid compounds. This interaction subsequently drives the oxidation process, leading to the formation of quinones, while concurrently facilitating the reduction of Ag$^+$ ions to Ag^0 [62,63]. This mechanism can be seen in the scheme of Fig. 5.

The presence of the AgNPs in the functionalized DE were corroborated by TEM analysis. The DE normal structure (Fig. 6 A) and a similar structure with the association of the NPs in the DEASE sample can be seen (Fig. 6 B and C). The NPs' morphology observed was quasispherical with an average size of 12 nm; the corresponding histogram in Fig. 6 D shows the most frequent size between 9 and 15 nm.

3.3. Antimicrobial assay

The results of the diffusion assay are presented in Fig. 7A. The

Functionalized diatomaceous earth (DES, DEAS, DESE and DEASE) was shown to be active against bacterial strains, with significant inhibition zones between 8 and 13 mm. *S. aureus* was the more sensitive bacterial strain and a photograph record can be seen in Fig. 7B. DE* and DE were not active against all the microorganisms tested.

The fungi were more resistant, especially *C. globosum* which showed growth inhibition only on the material (inhibition zone = 7) for the functionalized samples (DES, DEAS, DESE, DEASE), and can be considered as active, as can be seen in Fig. 7C. *A. alternata* was more sensitive to the functionalized DE without *E. giganteum* extract treatment (DES and DEAS). This could be related to the reduction of the Ag$^+$ ions to AgNPs, produced using plant extract in the DE* surface (DESE and DEASE), which would limit the possibility of Ag$^+$ ions leaching from the siliceous material. The Ag$^+$ ions that make contact with the culture medium in the diffusion assay can form soluble complexes with free organic molecules [64]. Additionally, the elevated humidity levels contribute to the potential leaching of these ions from the material.

Therefore, the activity against fungi could be developed through a mechanism of contact with the material, which would be more efficient than the lixiviation of the active agent considering the application on paints in the next step [65,66]. A general mechanism of antimicrobial activity of the coatings with the AgNPs is presented in Fig. 7D.

3.4. Paint characterization

The water absorption was not significantly modified after the addition of DE to the paint formulation, being 10.05% for CP and 9.15% for PDE. The same was registered with the water permeability, which after the first 24 h was 0.18 and 0.20 g/cm^2 for CP and PDE, respectively. This trend was maintained after 48 h (0.36 and 0.38 g/cm^2) and 72 h (0.61 and 0.58 g/cm^2). The specific weight was 1.41 g/cm^3 and it did not show a difference between one formulation and another, while the viscosity (U.K.) was 88.4 and 85.0 for CP and PDE, so slightly lower for the paint with DE. Finally, the hiding power was satisfactory for both paints with three layers of 75 μm for each. Therefore, this means that the addition of the DE (6.2 wt%) instead of the same amount of calcium
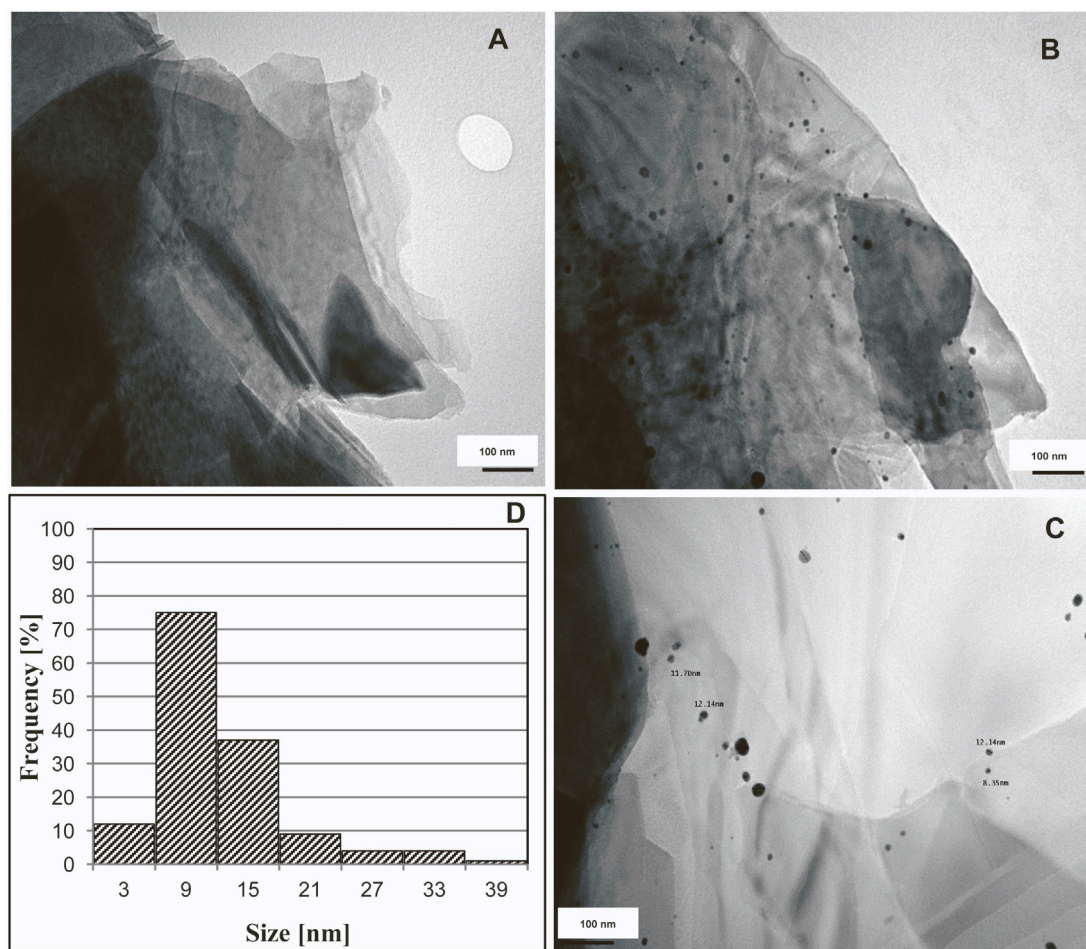
Fig. 6. TEM micrographs: (A) DE; (B and C) DEASE Magnification 270000x; (D) histogram that describes the sizes of the nanoparticles from DEASE sample.

carbonate did not significantly modify the properties of the paint. The ΔE of the coating due to the addition of DE was very evident ($\Delta E = 4.7$), while the gloss was 1.8 for both coatings of CP and PDE, within the standard for interior paints.

3.5. Resistance of paint films to microbial growth

The assessment of the fungal resistance of the coatings (CP, PDE, PDES, PDEAS, PDESE and PDEASE) was performed by a four week assay and the performance of the samples was rating (R) using the scale proposed by the ASTM D5590 standard. Paint films inoculated with *C. globosum* presented 100% inhibition (R = 0) for all the samples with functionalized DE (PDES, PDEAS, PDESE and PDEASE). *A. alternata* was the more resistance strain, with a higher degree of surface development, as corroborated by other published works [25,57]. This was attributed to the higher water requirements of *C. globosum* to grow (water activity > 0.9) compared to *A. alternata* (water activity < 0.9) [1]. Therefore controls (CP and PDE) showed heavy *A. alternata* growth (R = 4), while the paints with the functionalized DE presented a high degree of inhibition in all cases below light growth (R=2), as can be seen in Fig. 8. PDES and PDESE showed a color change, classified as very big, with values of 13.9 and 13.7 while those treated with the ammonia solution, PDEAS and PDEASE, decreased the ΔE value to 9.1 and 7.6, respectively, as can be corroborated in Fig. 8. In this sense, a higher color change could be related to the presence of pinkish Ag^+ ions [67]. This would indicate a more efficient reduction by adding the ammonia solution in the synthesis process, the AgNPs associated to the siliceous material are less prone to react and therefore more efficiently preserve the coating properties [27,68,69]. Especially, PDEASE achieved a very good

antifungal performance (R = 1, trace of growth) in addition to preserving the surface properties of the coating.

Although the degree of inhibition was high, it did not reach the 100% inhibition against *A. alternata*, as achieved in a previous research work on acrylic waterborne with free AgNPs (25 mg of Ag / 100 g of paint) obtained by a green synthesis with *Senna occidentalis* [57]. This could be due to a stronger retention of the nanoparticles by the siliceous material. The advantage of the present research was that a low concentration of the bioactive agent could be maintained with a good performance, which results in lower cost and a more eco-friendly product. On the other hand, a good retention of the AgNPs would allow a longer service life of the coating. The studied functionalized DEs present an advantage over commercial organic biocides that frequently lose their antimicrobial activity prematurely, shortening the useful life of the paint due to their low retention or degradation [70,71].

Others research works have shown different results depending not only on the concentration of AgNPs but also on the synthesis process and the structure of the support material. Machado et al. prepared waterborne acrylic paints with zeolite supported AgNPs (0.1 wt%) that proved be active against *Trichoderma harzianum* by a diffusion method [31]. Naik and Ratna synthesized a novel nanocomposite coating of hyperbranched urethane alkyd resin containing AgNPs, where the nanocomposite coating showed complete inhibition against *S. marcescens* at 0.5 wt% concentration of the AgNPs [72]. Tornedo et al. synthetized ZnO NPs associated with Ag NPs; antimicrobial trials showed a positive potential effect against different bacterial and fungal microorganisms as part of waterborne paint formulation (0.15 wt%) by diffusion assay, whilst against *Aspergillus niger* the maximum effect was obtained with a combination with other commercial biocides [30]. Farsinia et al.
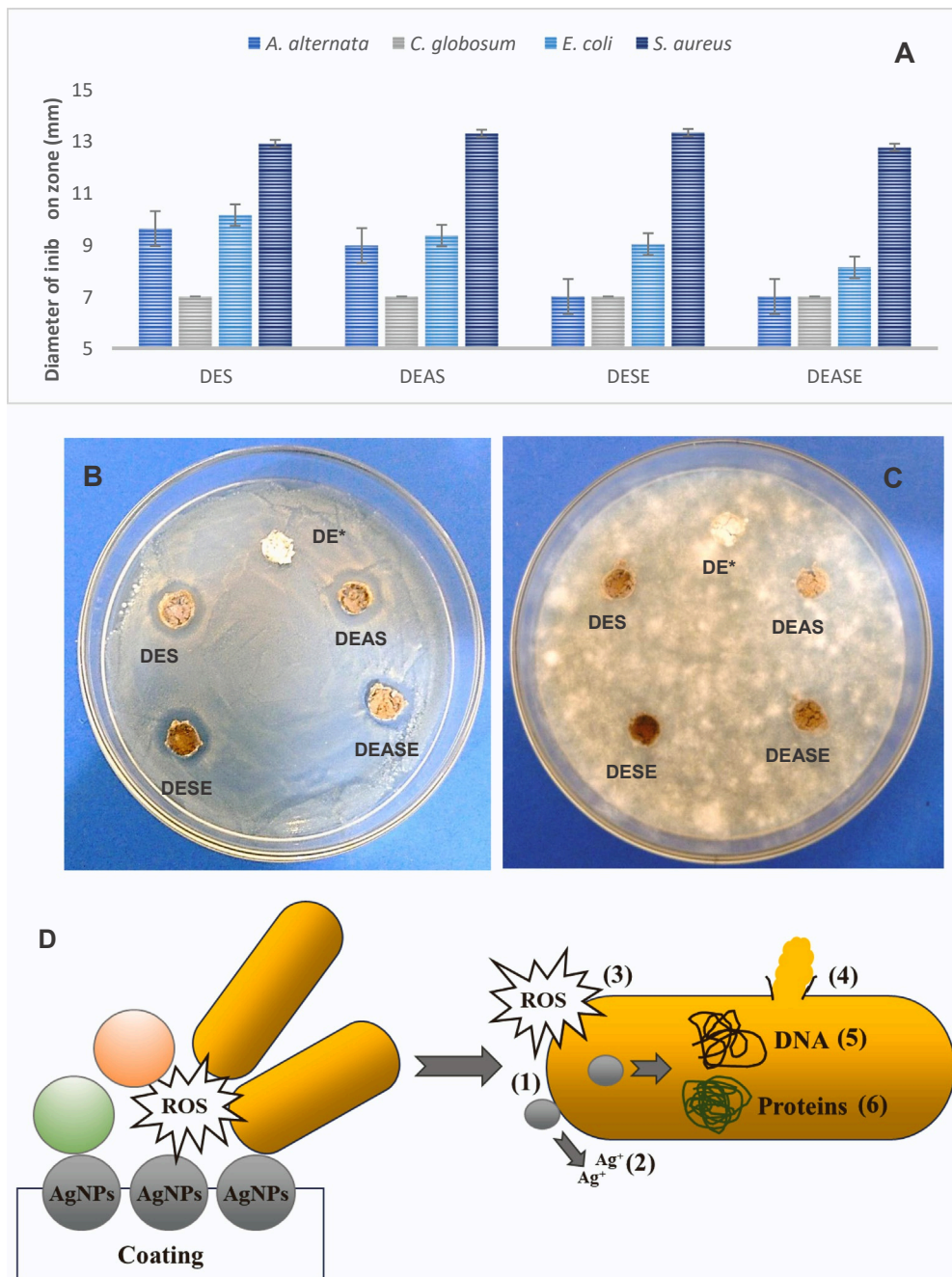
Fig. 7. Antimicrobial diffusion assay: (A) Bar graph presents the diameters of the inhibition halos of all samples against all strains tested; (B and C) photographs of the samples tested against *C. globosum* and *S. aureus*, respectively; (D) mechanism of antimicrobial activity on the coatings with AgNPs: (1) disruption of cell wall and plasma membrane components, (2) Ag^+ release affecting membrane proteins, (3) generation of reactive oxygen species (ROS), (4) leakage of cellular content, (5) nucleic acids damage, (6) protein deactivation.

synthesized a nanocomposite based on graphene associated to AgNPs (Ag-RGO) that was used as an additive to prepare antibacterial water-based acrylic paint, where the greatest reduction in *E. coli* colonies was obtained when the concentration of was 180 ppm [73]. Calovi et al. assessed colloidal silver in a polyurethane-based paint formulation, but did not improve the fungicidal activity against *Coniophora puteana* and *Trametes versicolor*, which was attributed to the low silver concentration (0.5 wt%) [74]. Arreche et al. synthetized by the sol-gel method additives associated with Ag to prepare acrylic waterborne paints (0.05 wt% Ag) and performed a four-week test in plates, resulting in total inhibition against *C. globosum*, with a lower degree of inhibition against *A. alternata* [68]. Similar results were obtained by the same

group when zirconia was incorporated in the sol-gel synthesis to associate Ag as additives in an acrylic paint [26]. In this sense, the use of DE is an advance, given its low cost compared to the materials obtained by the sol-gel method.

4. Conclusions

Functionalization of DE was achieved, obtaining a material associated with AgNPs by a green process that possessed antimicrobial activity. The addition of the DE does not modify the physical properties of the paint. The prepared waterborne acrylic paint proved to be resistant to mold spoilage and showed a high fungal inhibition. The results were
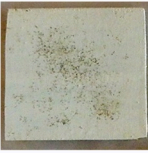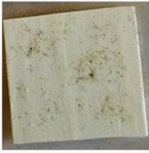
Fig. 8. Microbial resistance assay: photographs of samples exposed to *A. alternata* and rating (R).

improved to those obtained from sol-gel materials with AgNPs applied in paint formulation and, in addition to this, it is worth noting the very low cost of DE compared to sol-gel materials. For the first time *Equisetum giganteum* aqueous extract was employed for the nano-functionalization of DE. This kind of product could have applications in several industries, such as pharmaceutical, food and coating. Functionalized DE has the potential to prevent biodeterioration with 25 mg of silver per 100 g of paint, which is a very low concentration for a hygienic coating.

CRediT authorship contribution statement

Dra. Leyanet Barberia Roque: Conceptualization, Methodology, Investigation, Writing Original Draft, Dra. Marisa Viera: Conceptualization, Methodology, Supervision, Dra. Natalia Bellotti: Conceptualization, Methodology, Resources, Project, Administration; Writing-Review & Editing, Supervision, Funding acquisition.

Declaration of Competing Interest

The authors declare that they have no conflict of interest.

Data Availability

Data will be made available on request.

Acknowledgments

References

[1] O.C.G. Adan, R.A. Samson, Fundamentals of mold growth in indoor environments and strategies for healthy living, First, Wageningen Academic Publishers, The Netherlands, 2011, https://doi.org/10.3920/978-90-8686-722-6.

[2] C. Grant, C.A. Hunter, B. Flannigan, A.F. Bravery, The moisture requirements of moulds isolated from domestic dwellings, Int. Biodeterior. 25 (1989) 259–284, https://doi.org/10.1016/0265-3036(89)90002-X.

[3] N. Bellotti, C. Deyá, Waterborne functional paints to control biodeterioration, Handb. Waterborne Coat. (2020) 155–179, https://doi.org/10.1016/b978-0-12-814201-1.00007-x.

[4] M.A. Kakakhel, F. Wu, J.D. Gu, H. Feng, K. Shah, W. Wang, Controlling biodeterioration of cultural heritage objects with biocides: A review, Int. Biodeterior. Biodegrad. 143 (2019), https://doi.org/10.1016/j.ibiod.2019.104721.

[5] L. Song, J. Zhou, C. Wang, G. Meng, Y. Li, M. Jarin, Z. Wu, X. Xie, Airborne pathogenic microorganisms and air cleaning technology development: A review, J. Hazard. Mater. 424 (2022), 127429, https://doi.org/10.1016/j.jhazmat.2021.127429.

[6] World Health Organization, WHO Guidelines for indoor air quality: dampness and mould, ISBN 798 92 890 4168 3, (2009).

[7] E. Gámez-Espinosa, L. Barberia-Roque, N. Bellotti, Role of nanotechnology in the management of indoor fungi, Nanobiotechnology Diagnosis, Drug Deliv. Treat. (2020) 229–257, https://doi.org/10.1002/9781119671732.ch12.

[8] U.N. Habitat, UN-Habitat COVID-19 Policy and programme framework, ONU-Habitat (2020) 1–10. https://unhabitat.org/sites/default/files/2020/04/covid19_policy_and_programmatic_framework_eng-02.pdf%0A.

[9] P. Nguyen-Tri, T.A. Nguyen, P. Carriere, C. Ngo Xuan, Nanocomposite coatings: preparation, characterization, properties, and applications, Int. J. Corros. 2018 (2018) 1–19, https://doi.org/10.1155/2018/4749501.

[10] T. Jana, P.S. Maiti, T.K. Dhar, Development of a novel bio-based hybrid resin system for hygienic coating, Prog. Org. Coat. 137 (2019), 105311, https://doi.org/10.1016/j.porgcoat.2019.105311.

[11] K. Johns, Hygienic coatings: the next generation, Surf. Coat. Int. Part B Coat. Trans. 86 (2003) 101–110, https://doi.org/10.1007/BF02699620.

[12] M. Falkiewicz-Dulik, K. Janda, G. Wypych, Industrial Biocides, Handb. Mater. Biodegrad. Biostablization (2015) 33–65, https://doi.org/10.1016/b978-1-895198-87-4.50005-0.

[13] M. Ribeiro, L.C. Simões, M. Simões, Biocides, Encycl. Microbiol (2018) 478–490, https://doi.org/10.1016/B978-0-12-809633-8.12118-1.

[14] P. Dileep, S. Jacob, S.K. Narayanankutty, Functionalized nanosilica as an antimicrobial additive for waterborne paints, Prog. Org. Coat. 142 (2020), 105574, https://doi.org/10.1016/j.porgcoat.2020.105574.

[15] J. Hasan, R.J. Crawford, E.P. Ivanova, Antibacterial surfaces: the quest for a new generation of biomaterials, Trends Biotechnol. 31 (2013) 295–304, https://doi.org/10.1016/j.tibtech.2013.01.017.

[16] S. Hendessi, E.B. Sevinis, S. Unal, F.C. Cebeci, Y.Z. Menceloglu, H. Unal, Antibacterial sustained-release coatings from halloysite nanotubes/waterborne polyurethanes, Prog. Org. Coat. 101 (2016) 253–261, https://doi.org/10.1016/j.porgcoat.2016.09.005.

[17] P. Ganguli, S. Chaudhuri, Nanomaterials in antimicrobial paints and coatings to prevent biodegradation of man-made surfaces: a review, Mater. Today Proc. 45 (2020) 3769–3777, https://doi.org/10.1016/j.matpr.2021.01.275.

[18] S.M. Amorim, J. Suave, L. Andrade, A.M. Mendes, H.J. José, R.F.P.M. Moreira, Towards an efficient and durable self-cleaning acrylic paint containing mesoporous TiO2 microspheres, Prog. Org. Coat. 118 (2018) 48–56, https://doi.org/10.1016/j.porgcoat.2018.01.005.

[19] J.R. Morones, J.L. Elechiguerra, A. Camacho, K. Holt, J.B. Kouri, J.T. Ramírez, M.J. Yacaman, The bactericidal effect of silver nanoparticles, Nanotechnology 16 (2005) 2346–2353, https://doi.org/10.1088/0957-4484/16/10/059.

[20] S. Kumar, M. Singh, D. Halder, A. Mitra, Mechanistic study of antibacterial activity of biologically synthesized silver nanocolloids, Colloids Surf. A Physicochem. Eng. Asp. 449 (2014) 82–86, https://doi.org/10.1016/j.colsurfa.2014.02.027.

[21] E. Gámez-Espinosa, L. Barberia-Roque, O.F. Obidi, C. Deyá, N. Bellotti, Antifungal applications for nano-additives synthesized with a bio-based approach, Adv. Nat. Sci. Nanosci. Nanotechnol. 11 (2020), 015019, https://doi.org/10.1088/2043-6254/ab790f.

[22] B. Le Ouay, F. Stellacci, Antibacterial activity of silver nanoparticles: a surface science insight, Nano Today 10 (2015) 339–354, https://doi.org/10.1016/j.nantod.2015.04.002.

[23] C. Dominguez-Wong, G.M. Loredo-Becerra, C.C. Quintero-González, M.E. Noriega-Treviño, M.E. Compeán-Jasso, N. Niño-Martínez, I. Dealba-Montero, F. Ruiz, Evaluation of the antibacterial activity of an indoor waterborne architectural coating containing Ag/TiO2 under different relative humidity environments, Mater. Lett. 134 (2014) 103–106, https://doi.org/10.1016/j.matlet.2014.07.067.

[24] T.P.M. Ferreira, N.C. Nepomuceno, E.L.G. Medeiros, E.S. Medeiros, F.C. Sampaio, J.E. Oliveira, M.P. Oliveira, L.S. Galvão, E.O. Bulhões, A.S.F. Santos, Antimicrobial coatings based on poly(dimethyl siloxane) and silver nanoparticles by solution blow spraying, Prog. Org. Coat. 133 (2019) 19–26, https://doi.org/10.1016/j.porgcoat.2019.04.032.

[25] L. Barberia-Roque, E. Gámez-Espinosa, M. Viera, N. Bellotti, Assessment of three plant extracts to obtain silver nanoparticles as alternative additives to control biodeterioration of coatings, Int. Biodeterior. Biodegrad. 141 (2019) 52–61, https://doi.org/10.1016/j.ibiod.2018.06.011.

[26] R.A. Arreche, K. Igal, N. Bellotti, C. Deyá, P.G. Vázquez, Functionalized zirconia compounds as antifungal additives for hygienic waterborne coatings, Prog. Org. Coat. 128 (2019), https://doi.org/10.1016/j.porgcoat.2018.12.004.

[27] E. Abdullayev, K. Sakakibara, K. Okamoto, W. Wei, K. Ariga, Y. Lvov, Natural tubule clay template synthesis of silver nanorods for antibacterial composite coating characterization. FE-SEM images were acquired using a Hitachi S-4800 FE-SEM (accelerating voltage, 5 kV) to observe nanotube, ACS Appl. Mater. Interfaces 3 (2011) 4040–4046.

[28] R.D. Holtz, B.A. Lima, A.G. Souza Filho, M. Brocchi, O.L. Alves, Nanostructured silver vanadate as a promising antibacterial additive to water-based paints, Nanomed. Nanotechnol. Biol. Med 8 (2012) 935–940, https://doi.org/10.1016/j.nano.2011.11.012.

[29] P.C. Sahoo, F. Kausar, J.H. Lee, J.I. Han, Facile fabrication of silver nanoparticle embedded CaCO3 microspheres via microalgae-templated CO2 biomineralization: application in antimicrobial paint development, RSC Adv. 4 (2014) 32562–32569, https://doi.org/10.1039/c4ra03623a.

[30] A.C.F. Tornero, M.G. Blasco, M.C. Azqueta, C.F. Acevedo, C.S. Castro, S.J.R. López, Antimicrobial ecological waterborne paint based on novel hybrid nanoparticles of zinc oxide partially coated with silver, Prog. Org. Coat. 121 (2018) 130–141, https://doi.org/10.1016/j.porgcoat.2018.04.018.

[31] G.E. Machado, A.M. Pereyra, V.G. Rosato, M.S. Moreno, E.I. Basaldella, Improving the biocidal activity of outdoor coating formulations by using zeolite-supported silver nanoparticles, Mater. Sci. Eng. C 98 (2019) 789–799, https://doi.org/10.1016/j.msec.2019.01.040.

[32] A. Kumar, P.K. Vemula, P.M. Ajayan, G. John, Silver-nanoparticle-embedded antimicrobial paints based on vegetable oil, Nat. Mater. 7 (2008) 236–241, https://doi.org/10.1038/nmat2099.

[33] M. Zielecka, E. Bujnowska, B. Kępska, M. Wenda, M. Piotrowska, Antimicrobial additives for architectural paints and impregnates, Prog. Org. Coat. 72 (2011) 193–201, https://doi.org/10.1016/j.porgcoat.2011.01.012.

[34] R. Arreche, N. Bellotti, C. Deyá, P. Vázquez, Assessment of waterborne coatings formulated with sol-gel/Ag related to fungal growth resistance, Prog. Org. Coat. 108 (2017) 36–43, https://doi.org/10.1016/j.porgcoat.2017.04.007.

[35] R. Arreche, N. Bellotti, C. Deyá, P. Vázquez, Assessment of waterborne coatings formulated with sol-gel/Ag related to fungal growth resistance, Prog. Org. Coat. 108 (2017) 36–43, https://doi.org/10.1016/j.porgcoat.2017.04.007.

[36] G.D. da Silva, E.J. Guidelli, G.M. de Queiroz-Fernandes, M.R.M. Chaves, O. Baffa, A. Kinoshita, Silver nanoparticles in building materials for environment protection against microorganisms, Int. J. Environ. Sci. Technol. 16 (2019) 1239–1248, https://doi.org/10.1007/s13762-018-1773-0.

[37] L. Barberia-Roque, O.F. Obidi, E. Gámez-Espinosa, M. Viera, N. Bellotti, Hygienic coatings with bioactive nano-additives from Senna occidentalis-mediated green synthesis, NanoImpact 16 (2019), 100184, https://doi.org/10.1016/j.impact.2019.100184.

[38] E. Gámez-Espinosa, C. Deyá, M. Cabello, N. Bellotti, Tannin from Schinopsis balansae applied to the nanofunctionalization of protective antifungal coatings, Nano-Struct. Nano-Objects 27 (2021), 100770, https://doi.org/10.1016/j.nanoso.2021.100770.

[39] E.O. Ogunsona, R. Muthuraj, E. Ojogbo, O. Valerio, T.H. Mekonnen, Engineered nanomaterials for antimicrobial applications: a review, Appl. Mater. Today 18 (2020), https://doi.org/10.1016/j.apmt.2019.100473.

[40] P. Ganguli, S. Chaudhuri, Nanomaterials in antimicrobial paints and coatings to prevent biodegradation of man-made surfaces: a review, Mater. Today Proc. 45 (2020) 3769–3777, https://doi.org/10.1016/j.matpr.2021.01.275.

[41] M. Hasan, T. Saidi, A. Muyasir, Y.R. Alkhaly, M. Muslimsyah, Characteristic of calcined diatomaceous earth from Aceh Besar District - Indonesia as cementitious binder, IOP Conf. Ser. Mater. Sci. Eng. 933 (2020), 012008, https://doi.org/10.1088/1757-899X/933/1/012008.

[42] M. Hasan, A.D.D. Riski, T. Saidi, Husaini, P.N. Rahman, Flexural and splitting tensile strength of high strength concrete with diatomite micro particles as mineral additive, Defect Diffus. Forum 402 (DDF) (2020) 50–55, https://doi.org/10.4028/www.scientific.net/DDF.402.50.

[43] M. Hasan, T. Saidi, H. Husaini, Properties and microstructure of composite cement paste with diatomaceous earth powder (DEP) from Aceh Besar district – Indonesia, Asia-Pac. J. Sci. Technol. 27 (2022) 1–11, https://doi.org/10.14456/apst.2022.3.

[44] M. Hasan, A. Muyasir, T. Saidi, Husaini, R. Azzahra, Properties of high strength concrete with calcined diatomaceous earth as cement replacement under compression, Defect Diffus. Forum 402 (2020) 7–13, https://doi.org/10.4028/www.scientific.net/DDF.402.7.

[45] C. Lupu, M. Popescu, F. Oancea, Enhancement of Diatomaceous Earth Grain Protectant Activity by Essential Oils, (2020) 76. https://doi.org/10.3390/proceedings2020057076.

[46] M. Hasan, T. Saidi, M. Afifuddin, Mechanical properties and absorption of lightweight concrete using lightweight aggregate from diatomaceous earth, Constr. Build. Mater. 277 (2021) 122324, https://doi.org/10.1016/j.conbuildmat.2021.122324.

[47] M. Hasan, T. Saidi, Properties of blended cement paste with diatomite from Aceh Province Indonesia, IOP Conf. Ser. Mater. Sci. Eng. 796 (2020) 12034, https://doi.org/10.1088/1757-899X/796/1/012034.

[48] R.D. Crangle, Diatomite statistics and information, Nuevos Sist. Comun. e Inf. (2021) 2013–2015.

[49] C. Moale, M. Ghiurea, C.E. Sîrbu, R. Somoghi, T.M. Cioroianu, V.A. Faraon, C. Lupu, B. Trică, D. Constantinescu-Aruxandei, F. Oancea, Effects of siliceous natural nanomaterials applied in combination with foliar fertilizers on physiology, yield and fruit quality of the apricot and peach trees, Plants 10 (2021), https://doi.org/10.3390/plants10112395.

[50] X. Sun, J. Liu, Z. Zhang, Y. Zhi, L. Jin, J. Hang, L. Shi, One-step fabrication of wear-resistant superhydrophobic coating based on aminosilane-functionalized diatomaceous earth, J. Appl. Polym. Sci. 138 (2021) 1–14, https://doi.org/10.1002/app.51227.

[51] W. Liu, L. Zhuang, J. Liu, Y. Liu, L. Wang, Y. He, G. Yang, F. Shen, X. Zhang, Y. Zhang, Make the building walls always clean: A durable and anti-bioadhesive diatomaceous earth@SiO2 coating, Constr. Build. Mater. 301 (2021), 124293, https://doi.org/10.1016/j.conbuildmat.2021.124293.

[52] M.A. Fernández, N. Bellotti, Silica-based bioactive solids obtained from modified diatomaceous earth to be used as antimicrobial filler material, Mater. Lett. 194 (2017), https://doi.org/10.1016/j.matlet.2017.01.144.

[53] L. Barberia-Roque, E. Gámez-Espinosa, M. Viera, N. Bellotti, Assessment of three plant extracts to obtain silver nanoparticles as alternative additives to control biodeterioration of coatings, Int. Biodeterior. Biodegrad. 141 (2019), https://doi.org/10.1016/j.ibiod.2018.06.011.

[54] L.N. Francescato, S.L. Debenedetti, T.G. Schwanz, V.L. Bassani, A.T. Henriques, Identification of phenolic compounds in Equisetum giganteum by LC-ESI-MS/MS and a new approach to total flavonoid quantification, Talanta 105 (2013) 192–203, https://doi.org/10.1016/j.talanta.2012.11.072.

[55] M.A. Fernández, L. Barberia Roque, E. Gámez Espinosa, C. Deyá, N. Bellotti, Organo-montmorillonite with biogenic compounds to be applied in antifungal coatings, Appl. Clay Sci. 184 (2020), 105369, https://doi.org/10.1016/j.clay.2019.105369.

[56] N. Bellotti, R. Romagnoli, C. Quintero, C. Domínguez-Wong, F. Ruiz, C. Deyá, Nanoparticles as antifungal additives for indoor water borne paints, Prog. Org. Coat. 86 (2015) 33–40, https://doi.org/10.1016/j.porgcoat.2015.03.006.

[57] L. Barberia-Roque, O.F. Obidi, E. Gámez-Espinosa, M. Viera, N. Bellotti, Hygienic coatings with bioactive nano-additives from Senna occidentalis-mediated green synthesis, NanoImpact 16 (2019), https://doi.org/10.1016/j.impact.2019.100184.

[58] G.P. Lopez, M.V. Gallegos, M.A. Peluso, L.C. Damonte, J.E. Sambeth, N. Bellotti, ZnO recovered from spent alkaline batteries as antimicrobial additive for waterborne paints, Emergent Mater. 6 (2023) 147–158, https://doi.org/10.1007/s42247-022-00443-2.

[59] L.G. Ecco, S. Rossi, M. Fedel, F. Deflorian, Color variation of electrophoretic styrene-acrylic paints under field and accelerated ultraviolet exposure, Mater. Des. 116 (2017) 554–564, https://doi.org/10.1016/j.matdes.2016.12.051.

[60] M.C.A. Marcelo, D. Pozebon, M.F. Ferrão, Authentication of yerba mate according to the country of origin by using Fourier transform infrared (FTIR) associated with chemometrics, Food Addit. Contam. - Part A Chem. Anal. Control. Expo. Risk Assess. 32 (2015) 1215–1222, https://doi.org/10.1080/19440049.2015.1050702.

[61] T. Jasrotia, S. Chaudhary, A. Kaushik, R. Kumar, G.R. Chaudhary, Green chemistry-assisted synthesis of biocompatible Ag, Cu, and Fe2O3 nanoparticles, Mater. Today Chem. 15 (2020), 100214, https://doi.org/10.1016/j.mtchem.2019.100214.

[62] T.J.I. Edison, M.G. Sethuraman, Instant green synthesis of silver nanoparticles using Terminalia chebula fruit extract and evaluation of their catalytic activity on reduction of methylene blue, Process Biochem 47 (2012) 1351–1357, https://doi.org/10.1016/j.procbio.2012.04.025.

[63] E.A. Terenteva, V.V. Apyari, S.G. Dmitrienko, Y.A. Zolotov, Formation of plasmonic silver nanoparticles by flavonoid reduction: a comparative study and application for determination of these substances, Spectrochim. Acta - Part A Mol. Biomol. Spectrosc. 151 (2015) 89–95, https://doi.org/10.1016/j.saa.2015.06.049.

[64] A.C.F. Tornero, M.G. Blasco, M.C. Azqueta, C.F. Acevedo, C.S. Castro, S.J.R. López, Antimicrobial ecological waterborne paint based on novel hybrid nanoparticles of zinc oxide partially coated with silver, Prog. Org. Coat. 121 (2018) 130–141, https://doi.org/10.1016/j.porgcoat.2018.04.018.

[65] K. Bester, X. Lamani, Determination of biocides as well as some biocide metabolites from facade run-off waters by solid phase extraction and high performance liquid chromatographic separation and tandem mass spectrometry detection, J. Chromatogr. A 1217 (2010) 5204–5214, https://doi.org/10.1016/j.chroma.2010.06.020.

[66] C. Paijens, A. Bressy, B. Frère, R. Moilleron, Biocide emissions from building materials during wet weather: identification of substances, mechanism of release and transfer to the aquatic environment, Environ. Sci. Pollut. Res. 27 (2020) 3768–3791, https://doi.org/10.1007/s11356-019-06608-7.

[67] M.C. Chen, P.W. Koh, V.K. Ponnusamy, S.L. Lee, Titanium dioxide and other nanomaterials based antimicrobial additives in functional paints and coatings: review, Prog. Org. Coat. 163 (2022), 106660, https://doi.org/10.1016/j.porgcoat.2021.106660.

[68] R. Arreche, N. Bellotti, C. Deyá, P. Vázquez, Assessment of waterborne coatings formulated with sol-gel/Ag related to fungal growth resistance, Prog. Org. Coat. 108 (2017), https://doi.org/10.1016/j.porgcoat.2017.04.007.

[69] G.D. da Silva, E.J. Guidelli, G.M. de Queiroz-Fernandes, M.R.M. Chaves, O. Baffa, A. Kinoshita, Silver nanoparticles in building materials for environment protection against microorganisms, Int. J. Environ. Sci. Technol. 16 (2019) 1239–1248, https://doi.org/10.1007/s13762-018-1773-0.

[70] M. Edge, N.S. Allen, D. Turner, J. Robinson, K. Seal, The enhanced performance of biocidal additives in paints and coatings, Prog. Org. Coat. 43 (2001) 10–17, https://doi.org/10.1016/S0300-9440(01)00244-2.

[71] L.E. Mardones, M.S. Legnoverde, J.D. Monzón, N. Bellotti, E.I. Basaldella, Increasing the effectiveness of a liquid biocide component used in antifungal waterborne paints by its encapsulation in mesoporous silicas, Prog. Org. Coat. 134 (2019), https://doi.org/10.1016/j.porgcoat.2019.04.058.

[72] R.B. Naik, D. Ratna, Synthesis of silver nanoparticles embedded novel hyperbranched urethane alkyd-based nanocomposite for high solid antimicrobial

coating application, J. Coat. Technol. Res. 12 (2015) 1073–1083, https://doi.org/10.1007/s11998-015-9702-3.

[73] F. Farsinia, E.K. Goharshadi, N. Ramezanian, M.M. Sangatash, M. Moghayedi, Antimicrobial waterborne acrylic paint by the additive of graphene nanosheets/silver nanocomposite, Mater. Chem. Phys. 297 (2023), 127355, https://doi.org/10.1016/j.matchemphys.2023.127355.

[74] M. Calovi, V. Coroneo, S. Palanti, S. Rossi, Colloidal silver as innovative multifunctional pigment: the effect of Ag concentration on the durability and biocidal activity of wood paints, Prog. Org. Coat. 175 (2023), 107354, https://doi.org/10.1016/j.porgcoat.2022.107354.